SF_6 and its clusters in solid parahydrogen studied by infrared spectroscopy

Hiroyuki Katsuki, Takamasa Momose,[a] and Tadamasa Shida[b]
Division of Chemistry, Graduate School of Science, Kyoto University, Kyoto 606-8502, Japan and Japan Science and Technology Corporation (JST), Kyoto 606-8502, Japan

(Received 2 November 2001; accepted 20 February 2002)

The triply degenerate stretching vibration of sulfur hexafluoride and its clusters in solid parahydrogen at cryogenic temperatures is studied using Fourier transform infrared spectroscopy. The observed spectra are compared with theoretical spectra constructed on the basis of the intermolecular resonant dipole–dipole and the dipole–induced-dipole interactions. The absorptions due to monomer, dimer, trimer, and tetramer are discussed individually. © *2002 American Institute of Physics.* [DOI: 10.1063/1.1468883]

I. INTRODUCTION

Since the first observation of infrared photodissociation of a van der Waals (vdW) molecule by Scoles *et al.*,[1] numerous vdW molecules produced in a molecular beam have been studied with the use of photodissociation action spectroscopy.[2] Using sulfur hexafluoride (SF_6), Reuss and co-workers monitored the predissociation-induced intensity depletion of a beam of SF_6 clusters, interacting with tunable infrared laser radiation. They demonstrated that, in the dimer, the degenerate ν_3 vibrational band of SF_6 is split into a doublet, mainly because of the dynamical dipole–dipole interaction.[3–6] Similar studies were extended to the $(SiF_4)_2$ and $(SiH_4)_2$ systems and the spectral data were analyzed in terms of not only the dipole–dipole but also of the dipole–induced-dipole interactions.[5–8] Meanwhile, Urban and Takami observed the rotationally resolved spectra of $(SF_6)_2$ to conclude that the structure of the dimer is of D_{2h} symmetry.[9] Scoles *et al.* further developed a novel technique to study liquid helium droplets[10] and molecular hydrogen clusters[11] that incorporated SF_6 as a probe. The observed spectra were attributed to the monomer and the dimer of SF_6.[10,11] Subsequently, the rotational structure of the spectral feature reported by Scoles *et al.* was resolved by Toennies and co-workers by employing a continuously tunable laser.[12–16]

Guided by this work we have attempted to observe the vibrational absorption spectrum of SF_6 clusters in solid parahydrogen (p-H_2) at cryogenic temperatures. Solid parahydrogen is useful in matrix isolation spectroscopy because the intermolecular interaction between guest molecules and surrounding hydrogen molecules is very weak. This characteristic is demonstrated by our observation of the highly resolved rotation–vibration spectra of CH_4 and CD_4 in the p-H_2 matrix.[17–19] In the CH_4/p-H_2 system we found that the matrix-isolated CH_4 monomer exhibits fine spectral splittings which provide us with quantitative information on the subtle intermolecular interaction between the CH_4 molecule and the matrix.[20] Not only the isolated monomer but also clusters of CH_4 show a rather rich spectral structure[21] that indicates that the parahydrogen matrix is also useful for the study of molecular clusters.

Recently, Fajardo *et al.* observed the spectra of $(H_2O)_n/p$-H_2 for sizes up to the hexamer.[22] They reported the existence of a cyclic hexamer in the solid parahydrogen matrix in addition to the cage hexamer which is produced in a supersonic expansion. The cyclic hexamer of water had been reported in liquid helium droplets[23] but has never been found in the gas phase. The result of Fajardo *et al.* indicates the presence of a similarity between solid parahydrogen matrices and liquid helium droplets.

In the present work, our primary aim is to obtain the *direct* absorption spectrum of SF_6 and its clusters in solid p-H_2, rather than the photodissociation action spectrum in the molecular beam as in the previous studies. We expected rotationally resolved spectra for SF_6 monomers in solid p-H_2, as in the case of the CH_4/p-H_2 system. However, it turned out that such a molecular rotation was not found in the SF_6/p-H_2 system. This is reasonable because the rotational constant of SF_6, $B_{SF_6}=0.09$ cm^{-1}, is about one-fiftieth of the rotational constant of methane, $B_{CH_4}=4.8$ cm^{-1}. The large rotational constant of CH_4 allows the methane molecule to rotate almost freely to exceed the anisotropic potential barrier on account of the surrounding hydrogen molecules, while the small rotational constant of SF_6 may prevent the molecule from free rotation to exceed the similar or probably even higher potential barrier than that for CH_4. Despite this failure to obtain the rotationally resolved spectrum of SF_6, we have succeeded in procuring significant spectral information on SF_6 clusters of several sizes.

II. EXPERIMENTAL PARTS

A. Preparation of the sample and measurements

Solid SF_6/p-H_2 samples were prepared using two methods. One is the closed-cell method which was adopted in our previous work.[17,18] A brief recapitulation of this is as follows: A variable concentration gaseous mixture of SF_6 and p-H_2 was slowly introduced through a 1/16-inch stainless tube into a copper cell having a cavity of a diameter of 2.0 cm and an optical path length of 3.0 cm over a period of

[a]Author to whom correspondence should be addressed. Electronic mail: momose@kuchem.kyoto-u.ac.jp
[b]Present address: Kanagawa Institute of Technology, Atsugi 243-0292, Japan.

approximately 2.5 hours. Both ends of the cavity were sealed with BaF_2 windows with indium gaskets. The cell was attached to the flat base of a liquid helium cryostat with a temperature-controllable spacer. The temperature of the cell was set at 8.5 K to ensure optimum epitaxial growth of an optically transparent mixed crystal of $SF_6/p\text{-}H_2$. The growth of the crystal started from the surface of the cylindrical cavity toward the center of the copper cell. After the crystal was grown, the temperature was lowered from 8.5 K to 4.5 K, slowly enough to avoid cracking. From our previous work, it has been shown that the *c* axis of the crystal is approximately parallel to the radial direction of the round cylindrical copper cell.[18]

Another method of preparation of the solid $SF_6/p\text{-}H_2$ samples is the rapid-deposition method, developed by Fajardo *et al.*, to grow transparent matrices of hydrogen.[24,25] Although this rapid deposition does not guarantee the formation of neat epitaxial crystals (unlike the closed-cell method), we tried it because this method was deemed to be desirable for comparing the degree of isolation of the SF_6 molecules in the solid between slow and quick solidification. In the rapid deposition, an optical BaF_2 window was cooled to 2.9 K, which was the lowest attainable temperature in the present work. The gaseous mixture of $SF_6/p\text{-}H_2$ was sprayed onto the surface of the window to obtain $\sim$1 mm thick solid $SF_6/p\text{-}H_2$ samples in less than 20 min.

The optical measurement was carried out using a Bruker IFS-120HR Fourier-transform spectrometer with a spectral resolution of 0.25–0.01 cm^{-1}. An MCT (mercury–cadmium–telluride) detector was employed throughout the experiment.

B. Experimental results

Figures 1 and 2 show the representative spectra observed for the rapid deposition and the closed-cell deposition, respectively. In both figures, the top and the bottom spectra correspond to a lower and a higher ratio of concentration of SF_6 to $p\text{-}H_2$, respectively.

The molar ratios of $SF_6/p\text{-}H_2$ in the premixed gaseous samples in Fig. 1 were about 1×10^{-6} (top) and 1×10^{-4} (bottom) as estimated by the measurement of the pressure gauge. Similarly the ratios in Fig. 2 were 1×10^{-6} (top) and 1×10^{-5} (bottom). The above concentrations correspond to an upper limit of the concentrations in the solidified samples because part of the SF_6 molecules must be lost on the chill of the wall of the stainless tube during the introduction of the premixed gas into the cell or onto the BaF_2 window. In this present work, however, it is not necessary to know the exact concentrations in the solid samples, but we only need to compare the relatively dilute and concentrated samples prepared by both methods of solidification. We repeated these comparative spectral measurements to obtain similar spectral patterns as those shown representatively in Figs. 1 and 2.

III. SPECTRAL ASSIGNMENT

The monomeric SF_6 molecule in the gas phase shows the ν_3 asymmetric stretching vibrational absorption at around 948.0 cm^{-1}.[26] The absorption of the degenerate vibration

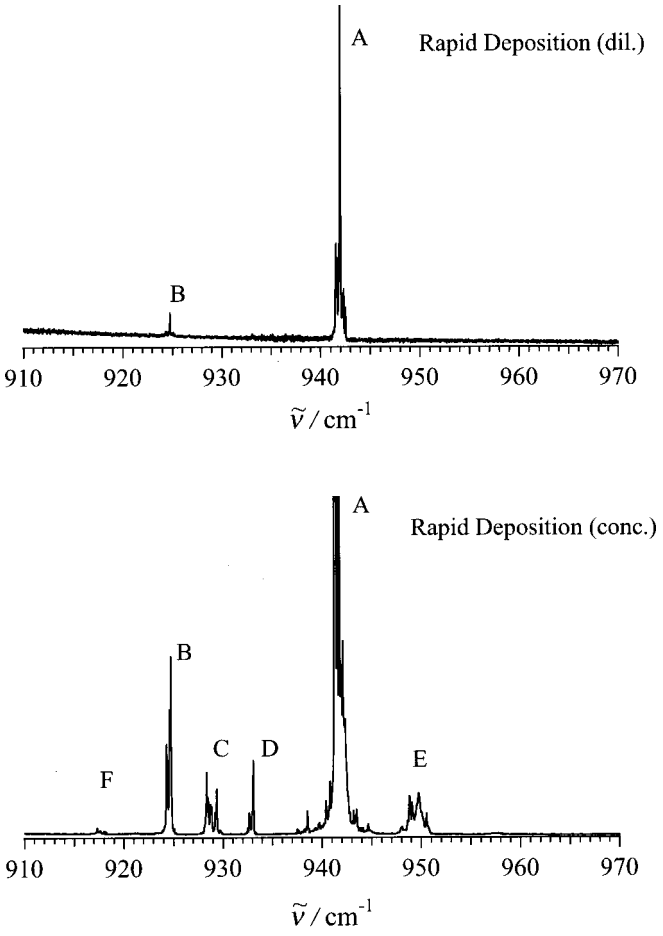

FIG. 1. Absorption spectra of the $SF_6/p\text{-}H_2$ system at 2.9 K formed by the rapid-deposition method. Top: the initial molar ratio of $SF_6/p\text{-}H_2$ in the premixed gas was 1×10^{-6}. Bottom: the ratio was about 1×10^{-4}.

splits into a doublet at about 934.0 and 956.1 cm^{-1} in the gaseous dimer.[9] Meanwhile, the monomeric SF_6 in liquid helium droplets exhibits the rotationally resolved ν_3 band at about 946.5 $\pm$ 0.1 cm^{-1}.[12,14] The shift of 948.0 cm^{-1} to 946.5 cm^{-1} between the gaseous SF_6 and SF_6 in helium droplets is quite small, which indicates that the perturbation due to the helium droplets is very weak. Monomers and dimers of SF_6 have also been studied in molecular hydrogen clusters.[11] In such clusters, the monomer absorption is located at 942.0 cm^{-1}, which is redshifted by 6.0 cm^{-1} relative to the gas phase value. The dimer shows a doublet at 928.5 and 949.6 cm^{-1}, comparable to the doublet at 934.0 and 956.1 cm^{-1} in the gas phase, but is redshifted by about 6 cm^{-1}, which is similar to the monomer shift.

On the basis of this reference data, we assign the major absorption of *A* at 942.0 cm^{-1} in the upper panel of Fig. 1 to monomeric $^{32}SF_6$ in solid $p\text{-}H_2$. We ignore for the moment the congested peaks flanking the absorption *A*. The minor absorption *B* is assigned to monomeric $^{34}SF_6$ as the intensity ratio is compatible with the ratio of the natural abundance of ^{32}S:$^{34}S\cong95.0$:4.2. Since the concentration ratio of SF_6 in the sample for the lower panel of Fig. 1 is higher than that in the upper panel by a factor of 10^2, the signal of the monomeric $^{32}SF_6$ (*A*) is out of scale, and that of $^{34}SF_6$ (*B*) is enhanced accordingly. The appearance of the new absorptions *C*, *D*, *E*,

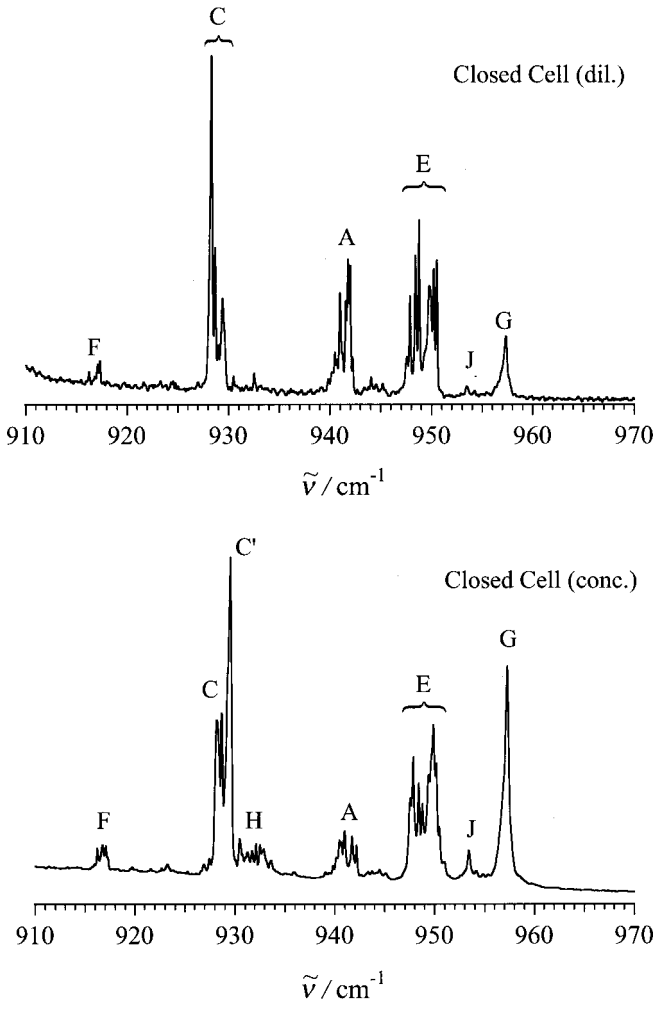

FIG. 2. Absorption spectra of the $SF_6/p\text{-}H_2$ system at 4.5 K formed using the closed-cell method. Top: The initial molar ratio of $SF_6/p\text{-}H_2$ in the premixed gas was about 1×10^{-6}. Bottom: The ratio was about 1×10^{-5}. During the crystallization, the cell was kept at 8.5 K and then cooled down to 4.5 K.

and *F* in the concentrated sample must be attributed to clusters of SF_6. Before considering these new absorptions we must first compare the general spectral patterns in Figs. 1 and 2, the latter being obtained for the samples prepared by the closed-cell method at 8.5 K and then kept at 4.5 K.

In Fig. 2, the absorptions *A* and *B* seen in Fig. 1 and assigned to the monomeric $^{32}SF_6$ and $^{34}SF_6$ are much reduced. The second point to note in Fig. 2 is that the absorptions *C*, *E*, and *F* seen in the concentrated sample of Fig. 1 are greatly enhanced in both spectra of Fig. 2. Looking at the fine structure of the absorption *C* in Fig. 2, we notice that in the concentrated sample there appears a strong, new absorption, labeled by *C′*, which behaves independently from *C*. The third difference between Figs. 1 and 2 is the appearance of intense absorption *G* and weak absorptions *H* and *J* in both spectra of Fig. 2. Further, the difference is in the substructures of the above-mentioned major absorptions.

The separations between *C* at 928.2–929.5 cm^{-1} and *E* at 947.5–950.5 cm^{-1} in both spectra of Fig. 2 are comparable to the doublet of *C* and *E* in Fig. 1. They are also comparable to the doublet of gaseous $(^{32}SF_6)_2$ at about 934.0 and 956.1 cm^{-1} if we assume a common redshift by about 6 cm^{-1} between the gas and the solid media.[3,4] The shift of 6 cm^{-1} is comparable to the difference between 942.0 cm^{-1} assigned to the monomeric $^{32}SF_6$ in $p\text{-}H_2$ solid and 948.0 cm^{-1} of the $^{32}SF_6$ molecule in the gas phase. Therefore, it is reasonable to conjecture that the absorptions *C* and *E* in Fig. 2 and in the lower spectrum of Fig. 1 are attributed to dimeric $^{32}SF_6$ in solid $p\text{-}H_2$. This is also supported by the results of the study of $^{32}SF_6$-doped H_2 clusters,[11] in which the dimer peaks are observed at 928.5 cm^{-1} and 949.6 cm^{-1}. The absorption *C′* is argued in the Discussion section.

As has been shown, the closed-cell method tends to form more clusters than the rapid-deposition method.[27] The higher temperature of 8.5 K in the closed-cell method than the temperature of 2.9 K in the rapid-deposition method during crystal growth may favor the cluster formation in the cell method. It was consistently observed that the absorption *A* assigned to the monomer in Fig. 2 decreased gradually when the closed-cell sample was kept at temperatures above 8.0 K. The above qualitative argument will be substantiated by an analysis of the intermolecular interaction among SF_6 molecules in the next section.

IV. ANALYSIS OF OBSERVED SPECTRA

A. General framework of analysis

The dominant mechanism for the splitting of the ν_3 band upon dimerization has been associated with the resonant dipole–dipole (DD) interaction.[4] The contribution of the additional dipole–induced-dipole (DID) interaction was also examined not only for $(SF_6)_2$ but also for the related systems of $(SiF_4)_2$ and $(SiH_4)_2$.[5] In the case of $(SF_6)_2$, it was concluded that the DD mechanism is dominant with only about a 10% contribution of the DID mechanism and that the contribution of the dispersion and the exchange interactions is negligible.[6,7]

In agreement with the preceding work, we also assume that only the DD and DID interactions are significant in the analysis of the observed spectra. Following the previous work,[4–7,9] we describe the triply degenerate ν_3 vibrational states of $(SF_6)_n$ $(n=2,3,...)$ in terms of $3\times n$ harmonic oscillator functions $|x_i\rangle$, $|y_i\rangle$, and $|z_i\rangle$ where the symbols such as $|x_i\rangle$ stand for the vibrational excited state in which the *x* component of the triply degenerate mode of the *i*th molecule is excited to the $v=1$ state. We consider the two Hamiltonians, shown in Eqs. (1) and (2) to describe the intermolecular interaction,

$$H_{\mathrm{DD}}=-\frac{1}{4\pi\epsilon_0}\sum_{i>j}\frac{3(\boldsymbol{\mu}_i\cdot\hat{\mathbf{R}}_{ij})(\boldsymbol{\mu}_j\cdot\hat{\mathbf{R}}_{ij})-\boldsymbol{\mu}_i\cdot\boldsymbol{\mu}_j}{R_{ij}^3}, \tag{1}$$

$$H_{\mathrm{DID}}=-\frac{1}{2}\,\frac{1}{(4\pi\epsilon_0)^2}\sum_{i,j\neq i}\frac{\alpha_i[\boldsymbol{\mu}_i\cdot\boldsymbol{\mu}_j+3(\boldsymbol{\mu}_j\cdot\hat{\mathbf{R}}_{ij})^2]}{R_{ij}^6}. \tag{2}$$

Here, the symbols $\boldsymbol{\mu}_i$ and α_i stand for the dipole operator and the isotropic polarizability of molecule *i*, respectively. The symbols R_{ij} and $\hat{\mathbf{R}}_{ij}$ represent the distance and the unit vector connecting the sulfur atoms in molecules *i* and *j*, respectively. Obviously, the diagonal elements of H_{DD} for the ground and for the $v=1$ vibrationally excited states vanish,

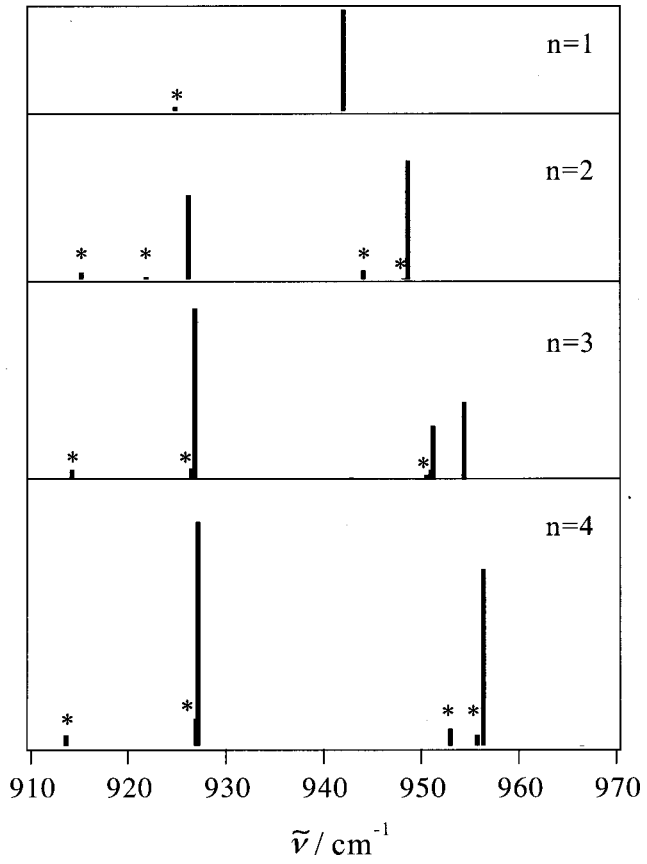

FIG. 3. Calculated stick spectra of the monomer and clusters up to tetramers. Trimers were assumed to have an equilateral triangular shape, and tetramers to have a regular tetrahedral shape. The absorption of mixed clusters containing a single $^{34}SF_6$, $(^{32}SF_6)_m(^{34}SF_6)$ are shown with asterisks. The parameters $\Delta_{DD}=7.05$ cm^{-1}, $\delta_{DID}=0.215$ cm^{-1}, $\omega_0(^{32}SF_6)=942.0$ cm^{-1}, and $\omega_0(^{34}SF_6)=924.8$ cm^{-1} were used for the calculation. The band origin ω_0 was assumed to be redshifted by 6 cm^{-1} from the gas phase values of $\omega_0^{gas}(^{32}SF_6)=948.0$ cm^{-1} and $\omega_0^{gas}(^{34}SF_6)=930.8$ cm^{-1}. The intensities of mixed clusters are reduced according to the relative abundance.

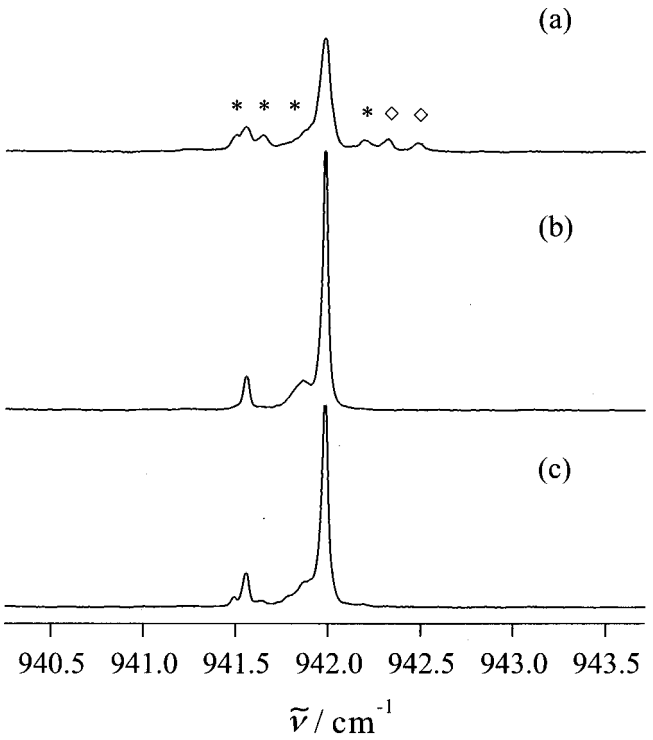

FIG. 4. Temperature dependence of the monomeric SF_6 observed for the rapid deposition. (a) Recorded at 2.9 K immediately after the deposition. (b) Recorded at 4.0 K after limited warming for 10 minutes at 4.0 K. (c) Recorded after cooling again at 2.9 K. Absorptions with asterisks were partially restored but those marked with ◇ disappeared irreversibly.

whereas the elements between the ground and the excited states give the nonzero transition dipole moment. As to the off-diagonal elements, only the terms of the kind, $\langle x_i|H_{DD}|x_j\rangle$, $\langle y_i|H_{DD}|y_j\rangle$, and $\langle z_i|H_{DD}|z_j\rangle$ survive. On the other hand, the diagonal elements of H_{DID} remains as nonzero for both the ground and the $v=1$ vibrational excited states of the dimer and larger clusters (see the matrix in Sec. IV C below).

The transition intensity is calculated from the dipole operator, which is given as the sum of the dipole operator of the jth molecule plus the induced dipole at molecule j by molecules k as in Eqs. (3) and (4).

$$\boldsymbol{\mu}_j=\boldsymbol{\mu}_j^0+\sum_k \boldsymbol{\mu}_{k\to j}^{\mathrm{ind}}, \tag{3}$$

$$\boldsymbol{\mu}_{k\to j}^{\mathrm{ind}}=\frac{\alpha}{4\pi\epsilon_0}\,\frac{-\boldsymbol{\mu}_k+3(\boldsymbol{\mu}_k\cdot\hat{\boldsymbol{R}}_{kj})\hat{\boldsymbol{R}}_{kj}}{R_{kj}^3}. \tag{4}$$

To a first order approximation, the dipole operator $\boldsymbol{\mu}_k$ appearing in Eq. (4) may be replaced with the operator $\boldsymbol{\mu}_k^0$, which is unaffected by molecules other than the kth.

B. Monomers

As is stated in Sec. III, the absorptions *A* and *B* are assigned to the monomeric $^{32}SF_6$ and $^{34}SF_6$ in solid p-H_2. The absorption *D* shown in the lower spectrum of Fig. 1 is assigned to monomeric $^{33}SF_6$ because the relative intensities *A*, *B*, and *D* are approximately proportional to the natural abundance of ^{32}S:^{34}S:$^{33}S=95.0$:4.2:0.8. In the top panel of Fig. 3 the calculated transition frequency of monomeric $^{32}SF_6$ is shown by the stick at 942.0 cm^{-1}, and that of $^{34}SF_6$ is shown with asterisk at 924.8 cm^{-1}. Both of them are shifted by -6 cm^{-1} from the gas phase values.

Each monomeric absorption is surrounded by congested substructures in a range of a few cm^{-1} around the absorption maxima. These structures cannot be associated with the rotational levels of the monomers, contrary to our initial anticipation by analogy with our work on the CH_4/p-H_2 system.[18,20] At the moment, we hypothesize that the substructures are related to multiple trapping sites, crystal field splitting, and the librational motion of the monomers in limited spatial environments. A temperature-dependent change of the substructures is given in Fig. 4 and is briefly commented upon in the Discussion section below.

C. Dimers

The $v=1$ triply degenerate ν_3 vibrational states are split in the dimer by H_{DD} and H_{DID}. The explicit 6×6 matrix is

$$
\begin{array}{c}
 \\
\langle x_1| \\
\langle y_1| \\
\langle z_1| \\
\langle x_2| \\
\langle y_2| \\
\langle z_2|
\end{array}
\begin{array}{c}
\begin{array}{cccccc}
|x_1\rangle & |y_1\rangle & |z_1\rangle & |x_2\rangle & |y_2\rangle & |z_2\rangle
\end{array} \\
\left(\begin{array}{cccccc}
\omega_1-14\delta_{\mathrm{DID}} & 0 & 0 & \Delta_{\mathrm{DD}} & 0 & 0 \\
0 & \omega_1-14\delta_{\mathrm{DID}} & 0 & 0 & \Delta_{\mathrm{DD}} & 0 \\
0 & 0 & \omega_1-20\delta_{\mathrm{DID}} & 0 & 0 & -2\Delta_{\mathrm{DD}} \\
\Delta_{\mathrm{DD}} & 0 & 0 & \omega_2-14\delta_{\mathrm{DID}} & 0 & 0 \\
0 & \Delta_{\mathrm{DD}} & 0 & 0 & \omega_2-14\delta_{\mathrm{DID}} & 0 \\
0 & 0 & -2\Delta_{\mathrm{DD}} & 0 & 0 & \omega_2-20\delta_{\mathrm{DID}}
\end{array}\right)
\end{array},
$$

where ω_1 and ω_2 are the fundamental vibrational frequencies of molecules 1 and 2, respectively. The symbols Δ_{DD} and δ_{DID} are defined as

$$\Delta_{\mathrm{DD}}=\frac{1}{4\pi\epsilon_0 R^3}|\mu_{01}|^2, \tag{5}$$

$$\delta_{\mathrm{DID}}=\frac{\alpha}{2(4\pi\epsilon_0)^2 R^6}|\mu_{01}|^2. \tag{6}$$

Here, the μ_{01} is the transition moment between the ground state and one of the vibrationally excited states. The symbol R is the distance between molecules in the dimer.

In the case of the dimer of the same isotopic species, such as $(^{32}SF_6)_2$ and $(^{34}SF_6)_2$, the fundamental frequencies ω_1 and ω_2 in the matrix above are the same. Thus, the corresponding eigenvalues and eigenvectors can be simply expressed below, where $\omega_0=\omega_1=\omega_2$,

eigenvalues	eigenvectors
$\omega_0-2\Delta_{\mathrm{DD}}-20\delta_{\mathrm{DID}}$	$\|1\rangle=\frac{1}{\sqrt{2}}(\|z_1\rangle+\|z_2\rangle)$
$\omega_0-\Delta_{\mathrm{DD}}-14\delta_{\mathrm{DID}}$	$\|2\rangle=\frac{1}{\sqrt{2}}(\|x_1\rangle-\|x_2\rangle),\|3\rangle=\frac{1}{\sqrt{2}}(\|y_1\rangle-\|y_2\rangle)$
$\omega_0+\Delta_{\mathrm{DD}}-14\delta_{\mathrm{DID}}$	$\|4\rangle=\frac{1}{\sqrt{2}}(\|x_1\rangle+\|x_2\rangle),\|5\rangle=\frac{1}{\sqrt{2}}(\|y_1\rangle+\|y_2\rangle)$
$\omega_0+2\Delta_{\mathrm{DD}}-20\delta_{\mathrm{DID}}$	$\|6\rangle=\frac{1}{\sqrt{2}}(\|z_1\rangle-\|z_2\rangle).$

(7)

In this case only the transitions to the eigenstates $|1\rangle, |4\rangle$, and $|5\rangle$ are allowed by symmetry where the states $|4\rangle$ and $|5\rangle$ are degenerated. The transition frequencies are given as the differences between the eigenvalues of $|1\rangle$ and $|4\rangle$ (or $|5\rangle$) and the ground state energy which is stabilized by dimerization to a value of $\langle 0|H_{\mathrm{DID}}|0\rangle=-12\delta_{\mathrm{DID}}$, where $|0\rangle$ represents the ground state. The right-hand side of Fig. 5 illustrates the energy levels of the ν_3 mode of the dimeric SF_6. It is seen that the perpendicularly polarized transition of the lower frequency is affected by the DID contribution by the amount of $|8\delta_{\mathrm{DID}}|$, while the contribution to the parallel transition of the higher frequency is $|2\delta_{\mathrm{DID}}|$.

The intensities of the allowed transitions are given by

$$\langle 0|\mu|1\rangle^2=\left|\left(1+\frac{2\alpha}{4\pi\epsilon_0 R^3}\right)\mu_{01}\right|^2, \tag{8}$$

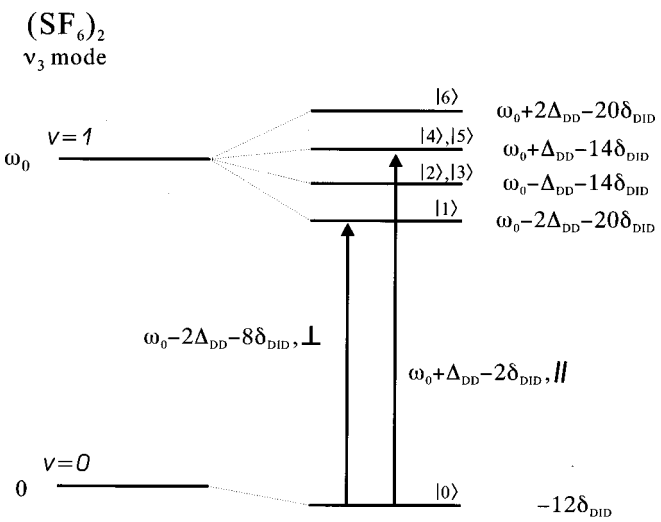

FIG. 5. Schematic energy level diagram of the ν_3 mode of SF_6 dimer.

$$\langle 0|\mu|4\rangle^2=\langle 0|\mu|5\rangle^2=\left|\left(1-\frac{\alpha}{4\pi\epsilon_0 R^3}\right)\mu_{01}\right|^2. \quad (9)$$

With the experimental polarizability of $\alpha/4\pi\epsilon_0=6.54$ Å^3 and the intersulfur distance of $R=4.754$ Å,[9] we obtain an intensity ratio

$$\frac{\langle 0|\mu|1\rangle^2}{\langle 0|\mu|4\rangle^2+\langle 0|\mu|5\rangle^2}=\frac{(1+0.12)^2}{2\times(1-0.06)^2}=0.71. \quad (10)$$

With this intensity ratio and with the values of $\Delta_{DD}=7.05$ cm^{-1}, $\delta_{DID}=0.215$ cm^{-1},[9] and $\omega_0=942.0$ cm^{-1}, the theoretical spectra of the dimer are constructed as shown in the second panel from the top of Fig. 3.

For the species ($^{32}SF_6$)($^{34}SF_6$), the fundamental frequencies ω_1 and ω_2 appearing in the matrix above are different, and thus the corresponding eigenvalues and eigenvectors become more complicated than Eq. (7) due to the broken symmetry of $\omega_1 \neq \omega_2$. There are four eigenvalues corresponding to two nondegenerate and two doubly degenerate states. In this case, all the four transitions have nonzero transition intensities. By assuming the values of $\omega_1=942.0$ cm^{-1} and $\omega_2=924.8$ cm^{-1}, we obtained four calculated sticks with asterisks in the second panel of Fig. 3. The abundance ratio of the homodimer and the heterodimer is calculated to be 1.0:0.09. The intensities of the heterodimer shown in Fig. 3 are reduced according to the natural abundance of ^{34}S against ^{32}S.

D. Larger clusters

The matrix in Sec. IV C for the dimer is expanded to 9×9 for the trimer. In addition, it becomes necessary to know the geometrical arrangements of the three SF_6 molecules. For simplicity, we assume that the shape of the trimer is an equilateral triangle with the same intersulfur distance of $R=4.754$ Å as that for the dimer.[9] The parameters of Δ_{DD} and δ_{DID} are also assumed to be the same as for the dimer. Thus, the spectrum of the trimer ($^{32}SF_6$)$_3$ is predicted to have three transitions at 926.8, 951.2, and 954.4 cm^{-1} as shown in the third panel from the top of Fig. 3. Preliminary calculations indicate that the transition frequencies and their intensities of trimer are sensitive to its geometry. In Fig. 3, another isotopic species of ($^{32}SF_6$)$_2$($^{34}SF_6$) is also taken into account with the proper weights related to the abundances.

Similar calculations are extended to tetramers [($^{32}SF_6$)$_4$ and ($^{32}SF_6$)$_3$($^{34}SF_6$)], assuming a regular tetrahedral conformation. The same parameters of R, Δ_{DD}, and δ_{DID} as those for the dimer and trimer are assumed. Figure 3 summarizes the theoretical spectra of clusters up to the tetramer.

V. DISCUSSION

The overall assignment of the experiments are given in Table I. The two major sticks for the dimer in the second panel of Fig. 3 are located at $\omega_0+\Delta_{DD}-2\delta_{DID}$ and $\omega_0-2\Delta_{DD}-8\delta_{DID}$, which correspond to the difference between the eigenvalues of Eq. (7) and the ground state energy of $-12\delta_{DID}$. Using the adopted parameters of Δ_{DD} and δ_{DID}, the two sticks are located at 926.1 and 948.6 cm^{-1}, which are close to the doublet of the dimer in molecular hydrogen clusters (928.5 and 949.6 cm^{-1}).[11] The doublet apparently corresponds to the two absorptions *C* and *E* shown in the lower spectrum of Fig. 1 and in both spectra of Fig. 2. The complicated structure of the absorptions *C* and *E* in Figs. 1 and 2 may be attributed to the possible coexistence of different configurations of the two $^{33}SF_6$ molecules and to the lift of the degeneracy of the excited state in the dimer.

TABLE I. Frequencies in units of cm^{-1} and assignment of observed spectra.

Obs.	Label	Assignment	Calc.[a]
916.0–917.0	*F*	$^{32}(SF_6)_m{}^{34}(SF_6)$ $m=1,2,3$	913.6–915.1
924.2–924.8	*B*	$^{34}SF_6$	924.8
928.2–929.5	*C*	$^{32}(SF_6)_2$	926.1
928.8–929.5	*C′*	$^{32}(SF_6)_3$ triangular (?)	926.8
		$^{32}(SF_6)_4$ tetrahedral	927.2
930.0–934.0	*H*	larger clusters ($n>4$)	
932.5–933.2	*D*	$^{33}SF_6$	
941.0–942.5	*A*	$^{32}SF_6$	942.0
947.5–950.5	*E*	$^{32}(SF_6)_2$	948.6
953.3	*J*	$^{32}(SF_6)_3{}^{34}(SF_6)$ tetrahedral	952.9
956.5–957.5	*G*	$^{32}(SF_6)_4$ tetrahedral	956.3

[a]The parameters are taken as $\Delta_{DD}=7.05$ cm^{-1}, $\delta_{DID}=0.215$ cm^{-1}, $\omega_0(^{32}SF_6)=942.0$ cm^{-1}, and $\omega_0(^{34}SF_6)=924.8$ cm^{-1}.

As stated above, the absorption *D* in Fig. 1 is regarded as due to the monomeric SF_6 which is detected on account of the enhanced concentration of SF_6. Thus, the spectral feature of the lower panel of Fig. 1 is explicable by invoking only the monomer and dimer.

In Fig. 2, the intensity of the monomer is drastically reduced and the dimer absorption becomes dominant to evenly reveal the heterodimer of ($^{34}SF_6$)($^{32}SF_6$), which is associated with the absorption *F* (cf. the leftmost stick with asterisk in the second panel of Fig. 3). In Fig. 2, the relative intensities of the absorptions *C* and *C′* vary drastically between the upper and lower spectra. The increase of the absorption *C′* in the concentrated sample indicates that it is associated with larger clusters, which is consistent with the theoretical spectra for $n=3$ and 4 in Fig. 3 and with the experimental results in helium droplets.[13]

The theoretical spectra in Fig. 3 also indicate that there are two fairly separated spectra in the trimer, but intense peaks that are approximately equal at 951.2 and 954.4 cm^{-1}. In contrast, the theoretical spectrum for the tetramer predicts a strong single absorption at 956.3 cm^{-1}. Although the calculated transition frequencies for the tetrahedral tetramer happen to agree with the observed absorptions *C′* and *G*, the correspondence between the calculated and the observed spectra for the trimer is poor. The simplified model of the trimer and other unknown causes may be responsible for the disagreement. The absorption *H* may reasonably be associated with larger clusters than the tetramer since we observed a drastic increase of its intensity in extremely concentrated samples.

Before concluding the discussion two brief comments will be made. One is the absorption of the triply degenerate bending mode (ν_4) of SF_6. We have surveyed the absorption in the 608–618 cm^{-1} region corresponding to the ν_4 mode. Figure 6 shows the spectrum observed for a sample in the closed-cell at a rather high ratio of 1.0×10^{-4}. It is found

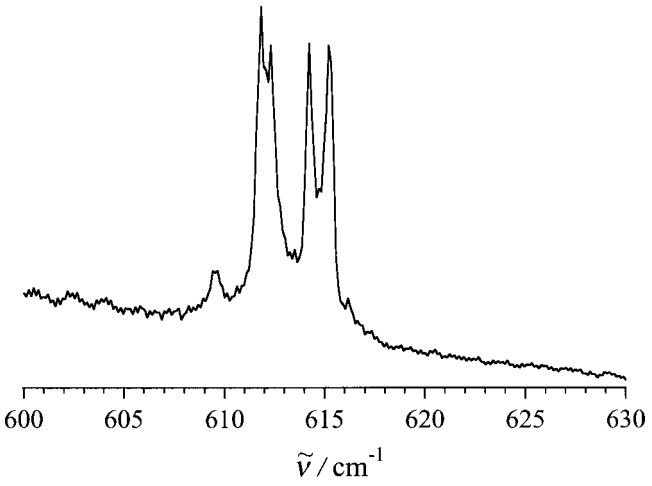

FIG. 6. Spectrum of the ν_4 vibrational transition of SF_6 clusters. The sample was prepared by the closed-cell method.

that the overall splitting of the ν_4 band is considerably smaller than that of the ν_3 band. The splitting of two dimer transitions is estimated to be 2.5 cm^{-1}. Comparing this value with the splitting of 21.5 cm^{-1} for the ν_3 band, we can estimate the ratio of transition moments $\mu_{01}(\nu_4)/\mu_{01}(\nu_3)$ to be 0.34 by the use of Eqs. (5)–(7). The transition dipole moments in the gas phase are reported to be 0.388 and 0.116 debye for the ν_3 and ν_4 bands, respectively.[28,29] From these data, the ratio of transition moments is calculated to be 0.30. The correspondence is fairly good considering the difference between the gas and solid phases.

The second point concerns the temperature dependence of the fine structure of the monomeric transition. The top panel of Fig. 4 shows an enlarged profile of the monomeric ($^{32}SF_6$) absorption observed for a sample prepared using the rapid-deposition method and maintained at 2.9 K. By changing the temperature from 2.9 K to 4.0 K, most of the structures disappeared (middle), but some of the substructures were partially restored when the sample was cooled again down to 2.9 K (below). The peaks marked with ◇ in the panel (a) of Fig. 4, which disappeared after the annealing, may be assigned to the monomeric SF_6 in the face-centered-cubic (fcc) phase. A similar spectral change due to the phase transition from the fcc phase to a hexagonal close-packed (hcp) phase has been observed with CH_4.[30] Other weak absorptions marked with asterisks in the panel (a) of Fig. 4 showed a change in reversible intensity between 2.9 K and 4.0 K. These absorptions became prominent only at 2.9 K. At the moment, we have no definite explanation for the spectral structures appearing only at the low temperatures.

In conclusion, it is emphasized that the direct absorption spectra of dimers and larger clusters are recorded and fairly well explained. The strong absorptions of the tetrahedral tetramer at about 957 cm^{-1} observed in the present work have not been reported previously in studies using liquid helium droplets.

ACKNOWLEDGMENTS

This work was supported in part by the Grant-in-Aid for Scientific Research of the Ministry of Education, Science, Culture, and Sports of Japan. H.K. acknowledges the support from JSPS Research Fellowships for Young Scientists.

[1] T. E. Gough, R. E. Miller, and G. Scoles, J. Chem. Phys. **69**, 1588 (1978).
[2] T. E. Gough, D. G. Knight, P. A. Rowtree, and G. Scoles, J. Phys. Chem. **90**, 4026 (1986).
[3] J. Geraedts, S. Setidi, S. Stolte, and J. Reuss, Chem. Phys. Lett. **78**, 277 (1981).
[4] J. Geraedts, S. Stolte, and J. Reuss, Z. Phys. A **304**, 167 (1982).
[5] M. Snels and J. Reuss, Chem. Phys. Lett. **140**, 543 (1987).
[6] B. Heijmen, A. Bizzarri, S. Stolte, and J. Reuss, Chem. Phys. **132**, 331 (1989).
[7] J. W. I. van Bladel and A. van der Avoird, J. Chem. Phys. **92**, 2837 (1990).
[8] D. Eichenauer and R. J. Le Roy, J. Chem. Phys. **88**, 2898 (1988).
[9] R. D. Urban and M. Takami, J. Chem. Phys. **103**, 9132 (1995).
[10] S. Goyal, D. L. Schutt, and G. Scoles, Phys. Rev. Lett. **69**, 933 (1992).
[11] S. Goyal, D. L. Schutt, G. Scoles, and G. N. Robinson, Chem. Phys. Lett. **196**, 123 (1992).
[12] R. Froechtenicht, J. P. Toennies, and A. Vilesov, Chem. Phys. Lett. **229**, 1 (1994).
[13] M. Hartmann, R. E. Miller, J. P. Toennies, and A. Vilesov, Science **272**, 1632 (1996).
[14] M. Hartmann, R. E. Miller, J. P. Toennies, and A. Vilesov, Phys. Rev. Lett. **75**, 1566 (1995).
[15] J. Harms, M. Hartmann, B. Sartakov, J. P. Toennies, and A. Vilesov, J. Chem. Phys. **110**, 5124 (1999).
[16] J. Harms, M. Hartmann, J. P. Toennies, A. Vilesov, and B. Sartakov, J. Mol. Spectrosc. **185**, 204 (1997).
[17] T. Momose and T. Shida, Bull. Chem. Soc. Jpn. **71**, 1 (1998), and references cited therein.
[18] T. Momose, M. Miki, T. Wakabayashi, T. Shida, M. C. Chan, S. S. Lee, and T. Oka, J. Chem. Phys. **107**, 7707 (1997).
[19] H. Hoshina, T. Wakabayashi, T. Momose, and T. Shida, J. Chem. Phys. **110**, 5728 (1999).
[20] T. Momose, J. Chem. Phys. **107**, 7695 (1997).
[21] T. Momose, H. Katsuki, H. Hoshina, N. Sogoshi, T. Wakabayashi, and T. Shida, J. Chem. Phys. **107**, 7717 (1997).
[22] M. E. Fajardo and S. Tam, J. Chem. Phys. **115**, 6807 (2001).
[23] K. Nauta and R. E. Miller, Science **287**, 293 (2000).
[24] S. Tam and M. E. Fajardo, Rev. Sci. Instrum. **70**, 1926 (1999).
[25] M. E. Fajardo and S. Tam, J. Chem. Phys. **108**, 4237 (1998).
[26] R. S. McDowell, J. P. Aldridge, and R. F. Holland, J. Phys. Chem. **80**, 1203 (1976).
[27] N. Sogoshi, Y. Kato, T. Wakabayashi, T. Momose, S. Tam, M. E. DeRose, and M. E. Fajardo, J. Phys. Chem. A **104**, 3733 (2000).
[28] K. Fox and W. B. Person, J. Chem. Phys. **64**, 5218 (1976).
[29] P. N. Schatz and D. F. Horning, J. Chem. Phys. **21**, 1516 (1953).
[30] S. Tam, M. E. Fajardo, H. Katsuki, H. Hoshina, T. Wakabayashi, and T. Momose, J. Chem. Phys. **111**, 4191 (1999).